

# Williams Syndrome

## Neuronal Size and Neuronal-Packing Density in Primary Visual Cortex

Albert M. Galaburda, MD; Dorothy P. Holinger, PhD; Ursula Bellugi, EdD; Gordon F. Sherman, PhD

**Background:** Williams syndrome (WMS) is a rare, genetically based syndrome associated with a hemideletion in chromosome 7 (7q11.22-23) and characterized by a unique constellation of somatic, brain, and cognitive features. Individuals with WMS demonstrate an unusual and uneven neuropsychological profile showing cognitive and visual spatial deficits juxtaposed with relative language preservation and excellent facial recognition.

**Objectives:** A neuroanatomical hypothesis for these behavioral findings suggests predominant involvement of the dorsal portions of the hemispheres relative to the ventral portions, including preferential involvement of peripheral visual field cortical representations over central representation. Predominant involvement of magnocellular visual pathways, as opposed to parvocellular pathways, is also suggested by this hypothesis.

**Subjects:** We examined primary visual cortical area 17 in the right and left hemispheres in 6 age- and sex-matched autopsy specimens from 3 WMS-affected brains (1 male and 2 females; mean [SD] age, 44 [14] years) and 3 control brains (1 male and 2 females; mean age, 43 [11] years).

**Design:** Neurons in layers II, III, IVA, IVB, IVC $\alpha$ , IVC $\beta$ , V, and VI were measured using an optical dissector method to determine possible differences between WMS-affected and control brains in cell-packing density, neuronal size, and neuronal size distribution.

**Results:** We found abnormalities in peripheral visual cortex in WMS-affected brains, but not in magnocellular subdivisions. There was a hemisphere by layer IV interaction and a layer IV left hemisphere and diagnosis interaction in cell-packing density. Williams syndrome-affected brains showed increased cell-packing density in left sublayer IVC $\beta$  and an excess of small neurons in left layers IVA, IVC $\alpha$ , IVC $\beta$ , V, and VI.

**Conclusions:** Cell measurements differ in peripheral visual cortical fields of WMS, with significantly smaller, more closely packed cells in some layers on the left side. These cell-packing density and neuronal size differences may be related to visuospatial deficits in this population.

*Arch Neurol.* 2002;59:1461-1467

From the Division of Behavioral Neurology, Departments of Neurology (Drs Galaburda and Holinger) and Psychiatry (Dr Holinger), Beth Israel Deaconess Medical Center and Harvard Medical School, Boston, Mass; Laboratory for Cognitive Neuroscience, The Salk Institute for Biological Studies, La Jolla, Calif (Dr Bellugi); and The Newgrange School Educational Outreach Center, Princeton, NJ (Dr Sherman).

**W**ILLIAMS syndrome (WMS), a mental retardation syndrome, consists of a unique constellation of somatic, brain, and cognitive features, and is associated with a hemideletion in the short arm of chromosome 7 (7q11.22-23).<sup>1-4</sup> At least 15 genes are associated with this hemideletion, which affects the same set of genes in nearly all clinically identified WMS. However, there are rare individuals with partial deletions with partial phenotypic manifestations of WMS.<sup>4,5</sup> Approximately 1 in 25 000 births exhibit the deletion and accompanying phenotype. Our histometric studies are part of a multidisciplinary project involving cognition, brain morphology (magnetic resonance imaging and functional magnetic resonance imaging), neurophysiology, and molecular genetics.

Specifically, our research has centered on the description of the neuroanatomical phenotype at the cytoarchitectonic,<sup>6-8</sup> histometric, and histochemical levels for the purpose of linking, on the one hand, brain change to behavior, and, on the other, brain change to the genomic anomaly.<sup>5,9</sup>

The microanatomical brain research in our laboratory is driven by a general hypothesis derived from the analysis of behaviors exhibited by individuals who have WMS. The WMS neuropsychological profile is an unusual and uneven one, consisting of deficits in processing visuospatial tasks, relative strength in many aspects of language, and a preserved ability to process human faces.<sup>9</sup> **Figure 1** shows the specific deficits in spatial cognition, deficits that are contrasted with comparable individuals with Down syndrome. Individuals who have WMS also demonstrate

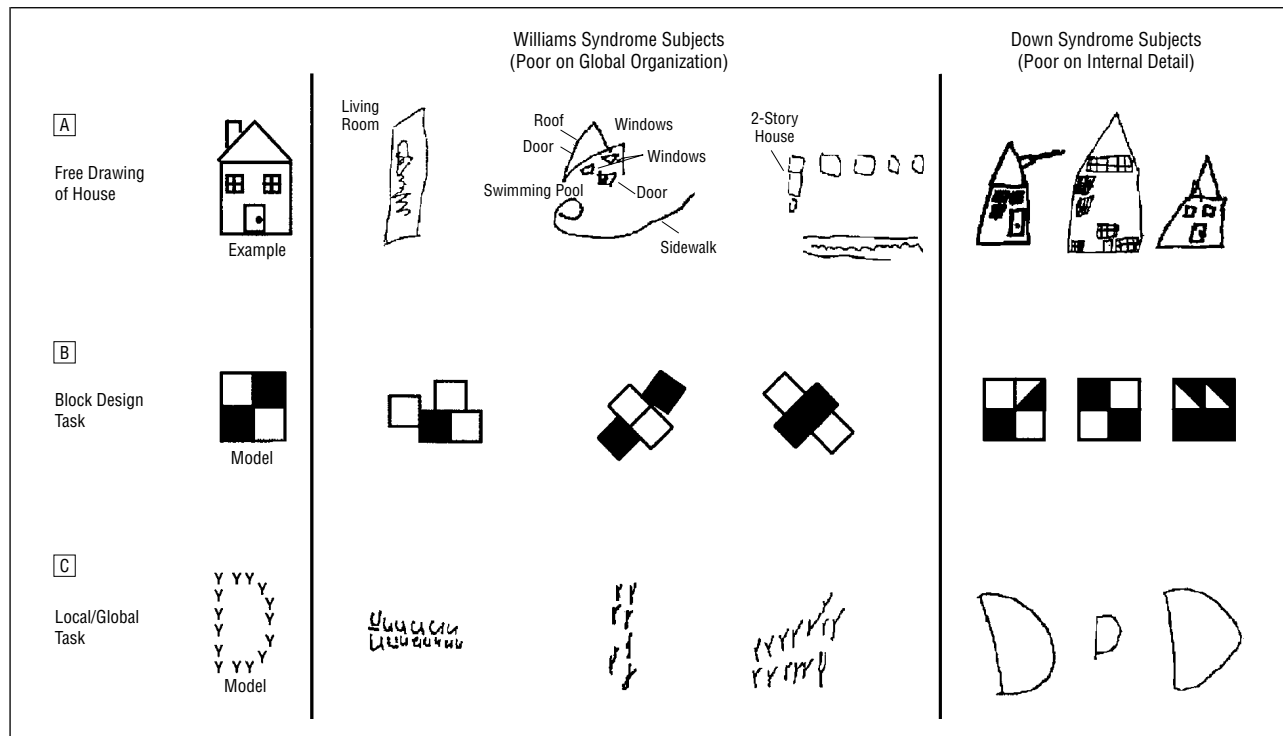


**Figure 1.** Note that both Williams syndrome-affected cases and Down syndrome-affected subjects are poor in spatial cognition, but in contrasting ways. Drawings and block designs of individuals with Williams syndrome tend to focus on the details at the expense of the whole, whereas individuals with Down syndrome tend to show global configuration but may be poor on internal detail. Reprinted with permission from *Trends in Neuroscience*.<sup>5</sup>

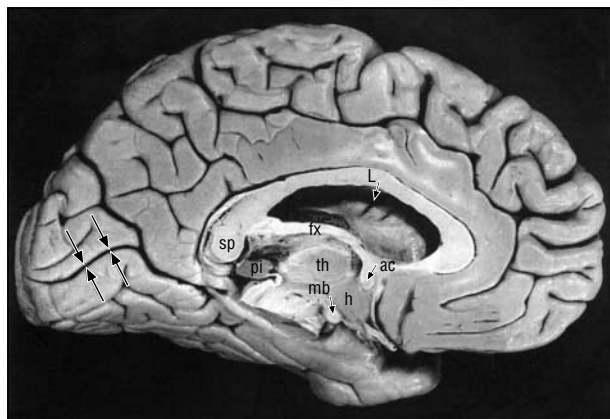


**Figure 2.** Blocks of tissue (7 × 5 × 5 cm) were taken from the medial surface of the left and right occipital lobes, dorsal and ventral to the calcarine sulcus (long arrows). sp indicates splenium; L, lateral ventricle; fx, fornix; pi, pineal gland; th, thalamus; ac, anterior commissure; mb, mamillary body; and h, hypothalamus. Reprinted with permission from Duvernoy HM. *The Human Brain, '91 Edition*. New York, NY: Springer-Verlag Wien, 1991:279.

an unusual personality characterized by a lack of fear of strangers, highly affective speech, and occasionally, inappropriate friendliness, and often show a great deal of interest in, and sometimes an ability regarding things musical.<sup>5,10</sup>

The best neuroanatomical fit for many of the behavioral findings seen in WMS seems to be the primary involvement of the dorsal portions of the hemispheres, which in the caudal half of the brain is concerned with representation and processing of visuospatial information<sup>11-14</sup> and in the frontal lobes with release and control of behavior.<sup>15</sup> By contrast, behaviors associated with the ventral and

perisylvian portions of the hemispheres, concerned with most aspects of language,<sup>16-18</sup> object properties of visual and other stimuli,<sup>19-21</sup> and programs for the performance of various motor behaviors (eg, speech<sup>22-23</sup>) seem to be at least relatively spared in WMS. Therefore, one part of the research in our laboratory has focused on comparing histometric features between the dorsal and ventral portions of the cerebral hemispheres. As part of a larger histometric study, we report herein a histometric analysis of the visual cortex of WMS. Specifically, we examined primary visual area 17 halfway between the splenium of the corpus callosum and the occipital pole along the calcarine sulcus (**Figure 2**); assuming normal topography of visual cortex in WMS, this sampled region would represent mostly peripheral fields pathways<sup>24-27</sup> and relates more to the dorsal visual pathway.<sup>11,28-29</sup>

## SUBJECTS AND METHODS

### SUBJECTS

We examined the visual cortex in age- and sex-matched autopsy specimens from 3 WMS-affected cases (1 male and 2 females; mean [SD] age, 44.0 [14] years) and from 3 neurologically and psychiatrically healthy control subjects (1 male and 2 females; mean age, 43.3 [11] years; the Harvard Brain Tissue Resource Center, McLean Hospital, Belmont, Mass). There was no information on handedness. The WMS cases had the 7q11.22-23 deletion determined by fluorescent in situ hybridization. The WMS-affected brains (1033 [104] g) were significantly smaller ( $P < .05$ ) than the control brains (1426 [177.8] g).

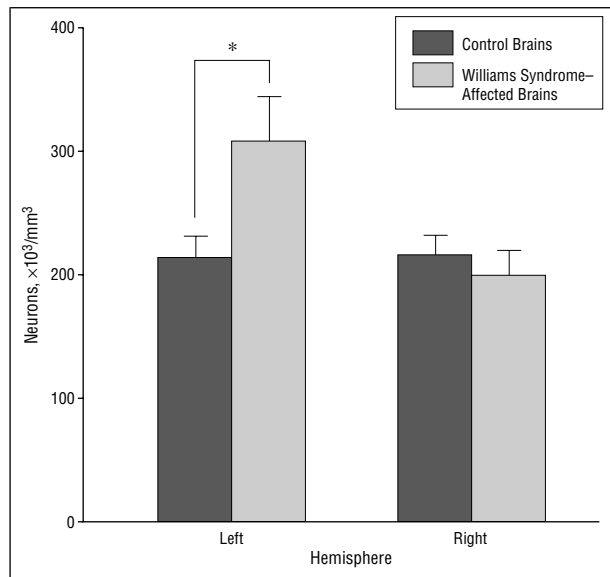


**Figure 3.** Cell-packing density in layer IVcβ of the left hemisphere was significantly increased in the Williams syndrome-affected brains compared with the control brains. Whereas in layer IVcβ of the right hemisphere, there was no significant difference between the 2 groups. Asterisk indicates  $P < .001$ .

#### HISTOLOGICAL STUDY

One WMS-affected brain (subject 1) was processed using the Yakovlev whole-brain method of serial histological sections.<sup>30</sup> The postmortem brain tissue from the remaining WMS-affected and control brains (subjects 2-6) was processed from left and right hemisphere blocks ( $7 \times 5 \times 5$  cm), including dorsal and ventral calcarine banks, and sectioned at  $30 \mu\text{m}$ . Every 10th section was stained with cresylechtviolett for Nissl substance.

#### AREA 17 CELL MEASURES

The primary visual cortex, area 17,<sup>31</sup> was easily identified in WMS-affected and control brains on the calcarine region. Three fields from the pial surface to the gray-white matter junction were selected where the plane of section was perpendicular or near perpendicular to the pial surface and there was no distortion by rippling, tears or other artifacts. All sections were coded so that the examiner was blind to diagnosis and hemisphere. The architectonic appearance of area 17 in WMS-affected brains is indistinguishable from that in controls, so this form of blinding was deemed to be adequate.

Layers II, III, IVA, IVB, IVcα, IVcβ, V, and VI of area 17 were measured in each hemisphere. Neurons were identified by the presence of a clearly visible, single nucleolus, a feature that distinguishes them from glial cells.<sup>32</sup> Cross-sectional neuronal areas and cell packing densities were measured using the modified dissector method and software of Williams and Rakic.<sup>33</sup> Using a universal microscope (Carl Zeiss Inc, Thornwood, NY) under  $\times 500$  oil magnification, images captured by a camera (Vidicon; Division of Hamamatsu USA, Bridgewater, NJ) were displayed on a monitor (model GVM 1310; Sony, Toronto, Ontario) that was connected to a personal computer workstation (Macintosh Centris 650; Apple Computers, Cupertino, Calif). The counting chamber ( $95 \times 85 \times 20 \mu\text{m}$ , at  $\times 500$ ) was placed within these images. A photoelectric micrometer (Heidenhain MP-25, Heidenhain, Schaumburg, Ill) interfaced to a National Instruments NB-GPIB card (NB-series cards, NB-GPIB IEEE-488.2, National Instruments Corp, Austin, Tex) in the Macintosh recorded movement in the z-axis. The base of

the sections was set to a z-axis reading of 0. A red opaque overlay precluded cell counting below the dimensions of the counting box. With the movement of the stage to  $5 \mu\text{m}$  ( $7.5 \mu\text{m}$  for subject 1) above the original position of the base of the section, the screen became transparent and the cells visible. The soma of the neurons were traced on a digitizing tablet, whereby neurons touching the top and left side of the screen were omitted. At a stage level of more than  $25 \mu\text{m}$  ( $27.5 \mu\text{m}$  for subject 1) above the original position of the base of the section, the screen turned opaquely green, which prevented the measurement of any cells above the optical counting box.

#### STATISTICAL ANALYSIS

Repeated-measures analysis of variance (ANOVA) was used to determine cell-packing density and neuronal size differences between the WMS and control cases. The independent measures included diagnosis (WMS and control), hemisphere (right and left), and layer (II, III, IVA, IVB, IVcα, IVcβ, V, and VI). The dependent measures were cell size (areas of the nucleus and cytoplasm together) and cell-packing density. The effect of sex could not be analyzed with any confidence because of the few cases studied. Differences in neuronal size distributions were analyzed using  $\chi^2$  tests.

### RESULTS

#### CELL-PACKING DENSITY

Repeated-measures ANOVA revealed significant differences in cell-packing density between the WMS-affected cases and controls and between hemispheres. As expected, based on the known difference in neuronal types among the layers, there was a significant effect of layer overall ( $F_{7,28} = 23.28$ ,  $P < .001$ ) and also for the left hemisphere ( $F_{7,28} = 27.42$ ,  $P < .001$ ) and the right hemisphere ( $F_{7,28} = 9.67$ ,  $P < .001$ ) separately. A hemisphere by layer interaction was significant only when layer IV (all sublaminae combined) was analyzed ( $F_{3,12} = 3.58$ ,  $P < .05$ ). Individual analyses of layers III and IV showed a significant increase in cell-packing density in the left hemisphere in the WMS-affected brains in sublayer IVcβ ( $F_{1,4} = 8.35$ ,  $P < .05$ ) compared with the controls ( $309598$  vs  $210526$  neurons/ $\text{mm}^3$ ) (**Figure 3**) but not in layer III. There was also a significant interaction between layer and diagnosis in the left hemisphere for layer IV ( $F_{3,12} = 3.58$ ,  $P < .05$ ), but not in the right hemisphere.

#### MEAN NEURONAL SIZE

Repeated-measures ANOVA analyses of cross-sectional mean neuronal areas did not result in any significant differences between WMS-affected and control brains. As expected, by the known differences in cell size between layers, there was a significant main effect of layer over both hemispheres ( $F_{7,28} = 20.63$ ,  $P < .001$ ) and for each hemisphere analyzed separately: left ( $F_{7,28} = 23.38$ ,  $P < .001$ ) and right ( $F_{7,28} = 11.11$ ,  $P < .001$ ).

#### NEURONAL SIZE DISTRIBUTIONS

Where there is marked variability in neuronal size, as is the case in the cerebral cortex, significant neuronal differences may be difficult to demonstrate, as in the case

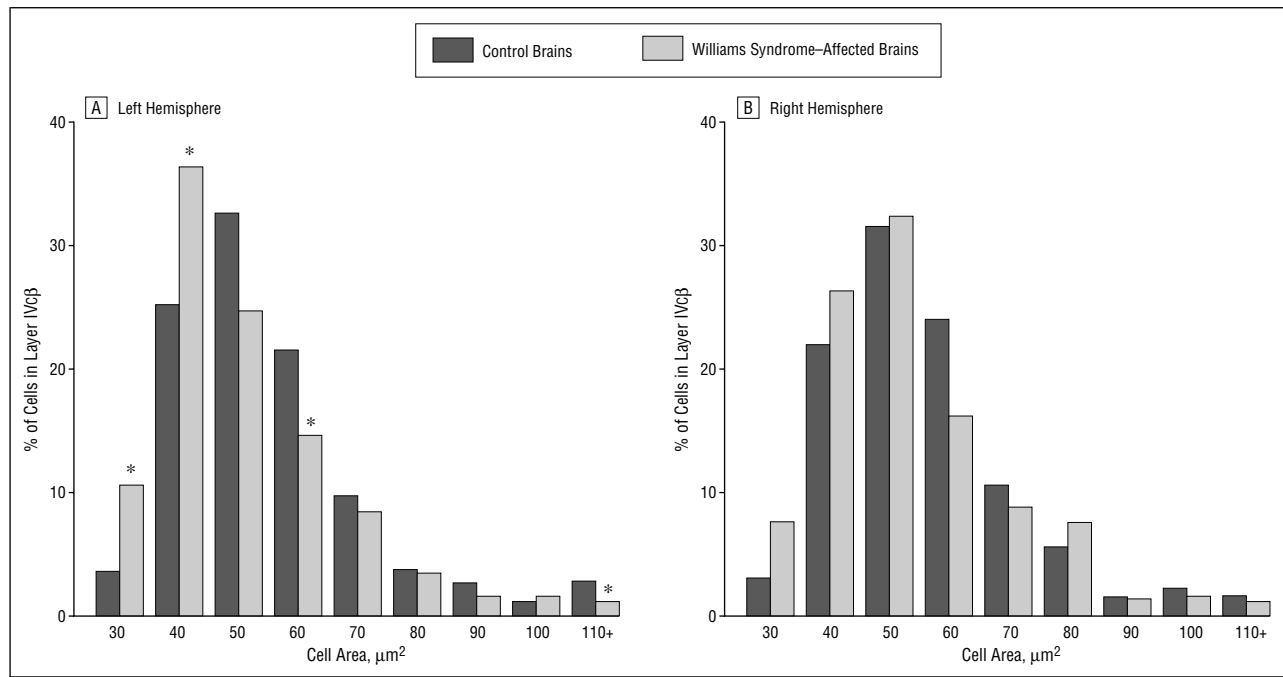


**Figure 4.** Layer IVcβ of the left and right hemispheres. A, There was a significant difference between the Williams syndrome-affected brains and the control brains ( $\chi^2_8=33.67$ ,  $P<.001$ ) with more small cells and fewer large cells in the Williams syndrome-affected brains compared with the control brains. Asterisks indicate  $P<.001$ . B, There were no significant differences between the 2 groups.

where both large and small neurons increase in numbers. Therefore, to assess additional differences in neuronal size in each layer and sublayer, we analyzed the frequency distribution of cell size in consecutive bins (**Figure 4**). The bins were arranged in ascending order of cell size. The number of bins ranged from 7 to 12, increasing by 10  $\mu\text{m}^2$ , and contained neurons whose size ranged from 30 to 90  $\mu\text{m}^2$ . We calculated  $\chi^2$  Values for the distribution of neurons in these bins between WMS-affected and control brains. We also examined distribution of cell size differences between hemispheres for WMS-affected and control brains separately. We set  $\alpha = .001$  for rejection of the null hypothesis to compensate for the high sensitivity of this test.

We examined each layer collapsed over both hemispheres between control and WMS-affected brains. There were significant differences for sublayers IVA ( $\chi^2_{10}=47.92$ ,  $P<.001$ ), IVcα ( $\chi^2_{11}=40.87$ ,  $P<.001$ ), IVcβ ( $\chi^2_8=54.04$ ,  $P<.001$ ), and for layers V ( $\chi^2_{11}=36.51$ ,  $P<.001$ ) and VI ( $\chi^2_{10}=31.34$ ,  $P<.001$ ). In each case, the most consistent finding was that WMS-affected brains had more small neurons than the control brains, whereas control brains had more large neurons. With an additional analysis of hemisphere, it was apparent that this effect was the result of differences in the left but not in the right hemisphere. When the hemispheres were analyzed separately, significant differences in the left hemisphere, but not the right, were found in sublayers IVA ( $\chi^2_7=32.48$ ,  $P<.001$ ), IVcα ( $\chi^2_8=31.08$ ,  $P<.001$ ), IVcβ ( $\chi^2_8=33.67$ ,  $P<.001$ ), and layers V ( $\chi^2_6=37.16$ ,  $P<.001$ ), and VI ( $\chi^2_{10}=33.09$ ,  $P<.001$ ). Again, this analysis showed the same pattern of more small neurons in the WMS-affected brains and more large neurons in the control brains (Figure 3 and 4A). When hemispheres were compared for cell size dis-

tribution, no significant asymmetries were seen in either WMS-affected or control brains.

#### COMMENT

In this study, we sought an anatomical explanation for the unique behavioral profile of individuals with WMS. For example, some behaviors are deeply abnormal while others are relatively preserved. Among the relatively preserved behaviors, we find language that is rich in vocabulary and affective prosody as well as excellent face recognition abilities and verbal memory.<sup>5,9,34,35</sup> More severely affected behaviors include visuospatial-visuomotor abilities and mathematics. As shown in Figure 1, individuals with WMS show specific deficits in spatial cognition tasks such as object assembly, block design, and drawing, suggesting difficulty with overall configurations.<sup>5,9,13</sup> Involvement of visuospatial functions implicates either the right hemisphere or the dorsal visual pathway,<sup>14,36</sup> whereas visual object recognition involves the left hemisphere or the ventral visual pathway.<sup>14</sup> In WMS-affected subjects, therefore, preservation of facial recognition abilities and affective speech prosody, which are linked to right hemisphere function, makes us suspect that the visuospatial and visuomotor deficits are not explained by a right hemisphere problem, but rather by a problem with the dorsal visual pathway and its connections to the motor system.<sup>37-40</sup> The present study was designed to test this hypothesis.

Based on anatomical, physiological, and clinical data, our hypothesis was that the abnormalities in WMS would be found in visual cortex that projects to the dorsal system (the part representing peripheral fields in the ante-

rior calcarine region), would affect neurons that form part of the magnocellular system, and would be more striking in the right hemisphere. The anterior calcarine cortex was sampled and, in fact, the findings were nearly the opposite. Specifically, although the peripheral visual cortex was found to be abnormal in WMS-affected brains, parvocellular sublayers in the left hemisphere only were involved.

In the primate visual system, there are structural and functional distinctions between 2 relatively segregated and independent processing pathways—the parvocellular and the magnocellular systems. These pathways have been characterized on the basis of anatomical,<sup>41</sup> psychophysical,<sup>42,43</sup> and physiological properties.<sup>28,44</sup> Neurons in these 2 systems differ in terms of receptive field size, sensitivity to color and light contrast, and timing properties. The parvo system is ideally suited for form, texture, and color analysis, while magno processes larger sections of space and appears better designed to calculate spatial location and motion. Anatomically, the magnoneurons are restricted to the lower 2 layers of the lateral geniculate nucleus, whereas parvo cells occupy the upper 4 layers. In the cortex, although a separation still exists (see below), it is less absolute.<sup>12,45</sup> For example, evidence from primate work suggests that segregation of magnocellular and parvocellular signals continue into extrastriate visual areas into higher-order visual processing. On the other hand, some primate studies suggest that magnocellular and parvocellular streams contribute differentially to dorsal and ventral pathways<sup>46</sup> and that V1 neurons integrate some information carried by both lateral geniculate nucleus magnocellular and parvocellular pathways.<sup>47</sup> Similarly, the visual system is subdivided into a dorsal and ventral pathway based on anatomical location and behavioral studies in monkeys and humans.<sup>11,14,46,48</sup> The relationship between the parvo-magno and dorsal-ventral subdivisions remains tentative<sup>49</sup> and also controversial,<sup>12</sup> but one may argue that the magnocellular system is the one more likely to contribute particularly to the dorsal visual system, with the parvo system contributing more specifically to the ventral system.<sup>43,50-51</sup> Also, based on clinical findings and activation studies, one would then be able to suggest that the magno system is not only dorsal but also lateralized to the right hemisphere, with the parvo system being lateralized to the left.<sup>14,36,48</sup> This suggestion is based on clinical observations that right hemisphere lesions tend to affect visuospatial abilities while left hemisphere lesions evince more clearly as visual object anomias and agnosias.<sup>52</sup> The findings of this study show that neuronal differences between WMS-affected cases and controls in primary visual cortex appear to affect the left hemisphere more than the right, particularly layer IV. Furthermore, the most consistent finding emerged in cell size distribution: WMS-affected visual cortex had more small and fewer large neurons than the control brains in layers IVA, IV $\alpha$ , IV $\beta$ , V, and VI of the left hemisphere. Williams syndrome-affected brains also showed increased cell-packing density in left layer IV $\beta$ . This layer receives inputs from the lateral geniculate nucleus. The lateral geniculate nucleus inputs to layer IV are sub-

laminar specific: layers IVA and IV $\beta$  receive projections from parvocellular layers of the lateral geniculate nucleus, whereas layers IVB and IV $\alpha$ <sup>28,46,50,53</sup> receive projections from magnocellular layers. However, the differences documented in this study in the visual cortex do not seem to respect magnocellular-parvocellular boundaries, as both IV $\alpha$  and IV $\beta$  are affected. On the other hand, although both IV $\alpha$  and IV $\beta$  show diminution in neuronal sizes, only IV $\beta$  has accompanying increased cell-packing density.

We also found that the size of the WMS-affected brains was significantly smaller than the healthy control brains ( $P < .05$ ), an observation also made in several structural magnetic resonance imaging studies.<sup>54</sup> Structural magnetic resonance imaging studies suggest that an important contributor to this reduction in size is diminished subcortical white matter.<sup>54-56</sup> There is also increased cortical folding<sup>54</sup> suggesting that, since the brain is reduced in size, it requires increased folding of the cortex to accommodate itself to the reduced core. On the other hand, an important source of the white matter is in fact the cortex, so reduction both of connectivity in the cortex and accompanying neuropil is also likely in a smaller brain. In this case, one would also expect that the reduced cortex in the WMS-affected brain should show some histometric changes. For instance, there may be fewer neurons. Conversely, the number of neurons could be relatively preserved, but the individual cell size is decreased and the cell-packing density is increased in accord with the reduction in the connectivity. Thus, we could interpret the present findings with reference not only to the healthy control brain, but also to what is expected given the reduction in overall brain size in those affected by WMS. Therefore, given our rationale that decreased cell size should be accompanied by increased cell-packing density in a smaller brain, the finding shown in IV $\alpha$ , which shows only decreased cell size but not increased cell-packing density, is also anomalous. It is possible, therefore, that this finding points to an added anomaly affecting the magnocellular visual system. One could not make this statement, however, without also saying that, even though packing densities appear normal in the suspected layers, the neurons must not function normally by virtue of abnormal, albeit not decreased, connectivity. Such a decrease in connectivity and neuropil may be a contributory mechanism for dysfunction in this system. One final point is that the decrease in white matter is compatible with the loss of long corticocortical connections, the main source of which is layer V pyramids and the main receptors of which is layer II. Excess of small neurons in layer V may indicate impoverished circuits affecting these long corticocortical connections, which are important for visuospatial functions.

## CONCLUSIONS

These conclusions are based on the assumption that the sampled area represents the peripheral visual fields in the WMS-affected brains and, thus, the dorsal visual pathways. We can be certain of this in the control brains, but less so in the WMS-affected cases. Thus, even though re-

cent maps of central vision show an expanded area subserving foveal vision<sup>26-27</sup> than earlier estimates,<sup>24-25</sup> we are certain to have sampled peripheral visual cortex in controls. However, if it were the case that central vision is even more expanded in WMS (which makes sense on theoretical grounds), it could be that, while we thought we were sampling peripheral visual cortex on topographic grounds, we were actually sampling cortex representing central vision in the WMS-affected cases. In that case the comparisons to the control samples would not be meaningful. While we cannot solve this conundrum—to ascertain the functional topography of the visual cortex—until functional activation studies are performed in WMS-affected subjects, our postmortem findings—more compaction and smaller cells in WMS-affected brains—may be related to the visuospatial deficits in this intriguing syndrome.

Accepted for publication March 7, 2002.

**Author contributions:** *Study concept and design* (Drs Galaburda and Holinger); *acquisition of data* (Drs Holinger and Bellugi); *analysis and interpretation of data* (Drs Galaburda, Holinger, Bellugi, and Sherman); *drafting of the manuscript* (Drs Holinger, Bellugi, and Sherman); *critical revision of the manuscript for important intellectual content* (Drs Galaburda, Holinger, and Sherman); *statistical expertise* (Drs Holinger and Sherman); *obtained funding* (Drs Galaburda and Bellugi); *administrative, technical, and material support* (Dr Galaburda); *study supervision* (Dr Galaburda); *graphics* (Dr Holinger).

The study was supported by grant HD33113 to the Salk Institute for Biological Studies from the National Institutes of Health, Bethesda, Md (Dr Bellugi). The brain tissue for controls was provided by the Harvard Brain Tissue Resource Center supported in part by grant MN/NS 31862 from the Public Health Service, Washington, DC.

We are grateful to the families who have donated the WMS-affected brains and to the local, regional, and national Williams Syndrome Associations. We appreciate technical assistance from Antis Zalkalns, BS.

Corresponding author and reprints: Albert M. Galaburda, MD, Beth Israel Deaconess Medical Center, 330 Brookline Ave, Boston, MA 02215 (e-mail: agalabur@caregroup.harvard.edu).

## REFERENCES

- Perez-Jurado LA, Wang YK, Peoples R, Coloma A, Cruces J, Francke U. A duplicated gene in the breakpoint regions of the 7q11.23 Williams-Beuren syndrome encodes the initiator binding protein TFII-I and BAP-135, a phosphorylation target of BTK. *Hum Mol Genet.* 1998;7:325-334.
- Wang YK, Samos CH, Peoples R, Perez-Jurado LA, Nusse R, Francke U. A novel human homologue of the *Drosophila* frizzled wnt receptor gene binds wingless protein and is in the Williams syndrome deletion at 7q11.23. *Hum Mol Genet.* 1997;6:465-472.
- Korenberg JR, Chen X-N, Lai Z, Yimlamia D, Bisighini R, Bellugi U. Williams syndrome: the search for the genetic origins of cognition. *Am J Hum Genet.* 1997;61:103.
- Korenberg JR, Chen XN, Hirota H, et al. VI. Genome structure and cognitive map of Williams syndrome. *J Cogn Neurosci.* 2000;12(suppl 1):89-107.
- Bellugi U, Lichtenberger L, Mills D, Galaburda A, Korenberg JR. Bridging cognition, the brain and molecular genetics: evidence from Williams syndrome. *Trends Neurosci.* 1999;22:197-207.
- Galaburda AM, Wang PP, Bellugi U, Rossen M. Cytoarchitectonic anomalies in a genetically based disorder: Williams syndrome. *Neuroreport.* 1994;5:753-757.
- Galaburda AM. In: Davidson RJ, Hugdahl K, eds. *Anatomical Basis of Cerebral Dominance.* Cambridge, Mass: MIT Press; 1995.
- Galaburda AM, Bellugi U. Multi-level analysis of cortical neuroanatomy in Williams syndrome. *J Cogn Neurosci.* 2000;12(suppl 1):74-88.
- Bellugi U, Lichtenberger L, Jones L, Lai Z, St George M. I. The neurocognitive profile of Williams syndrome: a complex pattern of strengths and weaknesses. *J Cogn Neurosci.* 2000;12(suppl 1):7-29.
- Levitin DJ, Bellugi U. Musical abilities in individuals with Williams syndrome. *Musical Perception.* 1998;15:357-389.
- Ungerleider LG, Mishkin M. Two cortical visual systems. In: Ingle DJ, Goodale MA, eds. *Analysis of Visual Behavior.* Cambridge, Mass: MIT Press; 1982.
- Tootell RB, Dale AM, Sereno MI, Malach R. New images from human visual cortex. *Trends Neurosci.* 1996;19:481-489.
- Atkinson J, King J, Braddick O, Nokes L, Anker S, Braddick F. A specific deficit of dorsal stream function in Williams' syndrome. *Neuroreport.* 1997;8:1919-1922.
- Shen L, Hu X, Yacoub E, Ugurbil K. Neural correlates of visual form and visual spatial processing. *Hum Brain Mapp.* 1999;8:60-71.
- Niki H, Watanabe M. Prefrontal and cingulate unit activity during timing behavior in the monkey. *Brain Res.* 1979;171:213-224.
- Damasio AR, Geschwind N. The neural basis of language. *Annu Rev Neurosci.* 1984;7:127-147.
- Fiez JA, Raichle ME. Linguistic processing. *Int Rev Neurobiol.* 1997;41:233-254.
- Raichle ME. What words are telling us about the brain. *Cold Spring Harb Symp Quant Biol.* 1996;61:9-14.
- Sergent J, Ohta S, MacDonald B. Functional neuroanatomy of face and object processing: a positron emission tomography study. *Brain.* 1992;115:15-36.
- Gauthier I, Tarr MJ, Moylan J, Skudlarski P, Gore JC, Anderson AW. The fusiform "face area" is part of a network that processes faces at the individual level. *J Cogn Neurosci.* 2000;12:495-504.
- Biederman I, Gerhardstein PC, Cooper EE, Nelson CA. High level object recognition without an anterior inferior temporal lobe. *Neuropsychologia.* 1997;35:271-287.
- Paus T, Perry DW, Zatorre RJ, Worsley KJ, Evans AC. Modulation of cerebral blood flow in the human auditory cortex during speech: role of motor-to-sensory discharges. *Eur J Neurosci.* 1996;8:2236-2246.
- Karis R, Horenstein S. Localization of speech parameters by brain scan. *Neurology.* 1976;26:226-233.
- Holmes G. Disruptions of vision by cerebral lesions. *Br J Ophthalmol.* 1918;2:353-384.
- Holmes G. The organization of the visual cortex in man. *Proc R Soc London Ser B.* 1945;132:348-361.
- Horton JC, Hoyt W. The representation of the visual field in human striate cortex: a revision of the classic Holmes map. *Arch Ophthalmol.* 1991;109:816-824.
- Engel SA, Glover GH, Wandell BA. Retinotopic organization in human visual cortex and the spatial precision of functional MRI. *Cereb Cortex.* 1997;7:181-192.
- Livingstone M, Hubel DH. Segregation of form, color, movement, and depth: anatomy, physiology, and perception. *Science.* 1988;240:740-749.
- Goodale MA, Milner AD. Separate visual pathways for perception and action. *Trends Neurosci.* 1992;15:20-25.
- Yakovlev PI. Whole-brain sections. In: Tedeschi CG, ed. *Neuropathology: Methods, Diagnosis.* Boston, Mass: Little Brown & Co; 1970:371-378.
- Brodman K. Vergleichende Lokalisationslehre der Grosshirnrinde in ihren prinzipien dargestellt auf grund des zellenbaues. Leipzig, Germany: JA Barth; 1909.
- Selemon LD, Rajkowska G, Goldman-Rakic PS. Abnormally high neuronal density in the schizophrenic cortex: a morphometric analysis of prefrontal area 9 and occipital area 17. *Am J Psychiatry.* 1995;52:805-818.
- Williams RW, Rakic P. Three-dimensional counting: an accurate and direct method to estimate numbers of cells in sectioned material. *J Comp Neurol.* 1988;278:344-352.
- Karmiloff-Smith A. Development itself is the key to understanding developmental disorders. *Trends Cogn Sci.* 1998;2:289-298.
- Losh M, Bellugi U, Reilly J, Anderson D. Narrative as a social engagement tool: the excessive use of evaluation in narratives from children with Williams syndrome. *Narrative Inquiry.* 2000;10:1-26.
- Corballis PM, Funnell MG, Gazzaniga MS. An evolutionary perspective on hemispheric asymmetries. *Brain Cogn.* 2000;43:112-117.
- Decety J, Perani D, Jeannerod M, et al. Mapping motor representations with positron emission tomography. *Nature.* 1994;371:600-602.

38. Iacoboni M, Woods RP, Brass M, Bekkering H, Mazziotta JC, Rizzolatti G. Cortical mechanisms of human imitation. *Science*. 1999;286:2526-2528.
39. Buccino G, Binkofski F, Fink GR, et al. Action observation activates premotor and parietal areas in a somatotopic manner: an fMRI study. *Eur J Neurosci*. 2001; 13:400-404.
40. Fogassi L, Gallese V, Buccino G, Craighero L, Fadiga L, Rizzolatti G. Cortical mechanism for the visual guidance of hand grasping movements in the monkey: a reversible inactivation study. *Brain*. 2001;124:571-586.
41. Livingstone MS, Hubel DH. Connections between layer 4B of area 17 and thick cytochrome oxidase stripes of area 18 in the squirrel monkey. *J Neurosci*. 1987; 7:3371-3377.
42. Livingstone MS, Rosen GD, Drislane FW, Galaburda AM. Physiological and anatomical evidence for a magnocellular defect in developmental dyslexia. *Proc Natl Acad Sci U S A*. 1991;18:7943-7947.
43. Galaburda AM, Livingstone M. Evidence for a magnocellular defect in developmental dyslexia. *Ann N Y Acad Sci*. 1993;682:70-82.
44. Shapley R. Parallel pathways in the mammalian visual system. *Ann N Y Acad Sci*. 1982;388:11-20.
45. Lachica EA, Beck PD, Casagrande VA. Parallel pathways in macaque monkey striate cortex: anatomically defined columns in layer III. *Proc Natl Acad Sci U S A*. 1992;89:3566-3570.
46. Sawatari A, Callaway EM. Convergence of magno- and parvocellular pathways in layer 4B of macaque primary visual cortex. *Nature*. 1996;380:442-446.
47. Allison JD, Meltzer P, Ding Y, Bonds AB, Casagrande VA. Differential contributions of magnocellular and parvocellular pathways to the contrast response of neurons in bush baby primary visual cortex (V1). *Vis Neurosci*. 2000;17: 71-76.
48. Haxby JV, Grady CL, Horwitz B, et al. Dissociation of object and spatial visual processing pathways in human extrastriate cortex. *Proc Natl Acad Sci U S A*. 1991;88:1621-1625.
49. Mishken M, Ungerleider LG, Macko KA. Object vision and spatial vision. *Trends Neurosci*. 1983;6:414-417.
50. Merigan WH, Maunsell JH. How parallel are the primate visual pathways? *Annu Rev Neurosci*. 1993;16:369-402.
51. Wong-Riley MTT. Primate visual cortex. In: Peters A, Rockland KS, eds. *Cerebral Cortex: Primary Visual Cortex in Primates*. New York, NY: Plenum Publishing Corp; 1994:141-193.
52. Farah MJ, Feinberg TE. *Visual Object Agnosia*. In: Feinberg TE, Farah MJ, eds. New York, NY: McGraw-Hill Co; 1997.
53. Casagrande VA, Norton TT. The lateral geniculate nucleus: a review of its physiology and function. In: Leventhal AG, ed. *The Neural Basis of Visual Function*. New York, NY: Macmillan Publishing Co Inc; 1991.
54. Schmitt JE, Eliez S, Bellugi U, Reiss AL. Analysis of cerebral shape in Williams syndrome. *Arch Neurol*. 2001;58:283-287.
55. Jernigan T, Bellugi U. Anomalous brain morphology on magnetic resonance images in Williams syndrome and Down syndrome. *Arch Neurol*. 1990;47:529-533.
56. Reiss A, Eliez S, Schmitt JE, et al. IV. Neuroanatomy of Williams syndrome: a high-resolution MRI study. In: Bellugi U, St George M, eds. *J Cogn Neurosci*. 2000;12(suppl 1):65-73.

### Correction

**Error in Abstract.** In the article titled "Stroke or Transient Ischemic Attacks With Basilar Artery Stenosis or Occlusion," published in the April issue of the ARCHIVES (2002;59:567-573), the third line of the "Patients and Methods" section should have read ". . . caused by BAS greater than 50%. . ."